Journal of Alloys and Compounds 506 (2010) 160–166

Contents lists available at ScienceDirect

Journal of Alloys and Compounds

journal homepage: www.elsevier.com/locate/jallcom

Influence factors on electrochemical properties of $Li_4Ti_5O_{12}$/C anode material pyrolyzed from lithium polyacrylate

Xuebu Hu[a,d], Ziji Lin[b,c], Kerun Yang[b,c], Zhenghua Deng[b,c,d,*], Jishuan Suo[b,c]

[a] Department of Chemistry and Materials, Sichuan Normal University, Chengdu, Sichuan 610068, PR China
[b] Chengdu Institute of Organic Chemistry, Chinese Academy of Sciences, Chengdu, Sichuan 610041, PR China
[c] Graduate School of Chinese Academy of Sciences, Beijing 100039, PR China
[d] Zhongke Laifang Power Science & Technology Co., Ltd, Chengdu, Sichuan 610041, PR China

ARTICLE INFO

Article history:
Received 11 August 2009
Received in revised form 29 June 2010
Accepted 30 June 2010
Available online 7 July 2010

Keywords:
$Li_4Ti_5O_{12}$/C
Influence factors
Lithium polyacrylate
Solid-state reaction
Electrochemical properties

ABSTRACT

Spinel $Li_4Ti_5O_{12}$/C was synthesized by one-step solid-state reaction route using lithium polyacrylate (PAALi) as lithium and carbon sources, and TiO_2 as titanium source. The characteristics of $Li_4Ti_5O_{12}$/C composites were determined by X-ray diffraction, scanning electron microscopy, transmission electron microscopy and thermogravimetric-differential thermal analysis methods. Their electrochemical performances were investigated by cyclic voltammograms, constant current charge–discharge and rate charge–discharge. It was found that molecular weight of polyacrylic acid (PAA), heating rate and sintering duration directly affected the physical and electrochemical performances of $Li_4Ti_5O_{12}$/C composites. The $Li_4Ti_5O_{12}$/C composites with the optimized electrochemical performances were obtained in the following conditions, i.e., PAA with the molecular weight of 10,000, heating rate of 20 °C min^{-1} and sintering duration of 8 h. At charge–discharge rate of 4 C and 8 C, the optimized sample showed discharge capacities of 148.4 and 142.4 mAh g^{-1}, with capacity retention of 94.48 and 90.53% after 50 cycles, respectively. Even at 20 C, its discharge capacity was 116.0 mAh g^{-1} with capacity retention of 87.61% after 50 cycles.
© 2010 Elsevier B.V. All rights reserved.

1. Introduction

Lithium-ion battery has developed rapidly in the past decades due to growing needs of electronic and information industries. Nowadays, the demand for lithium-ion batteries is still increasing and safety requirements are higher and higher. Therefore, exploration of a new anode material that is high safety and excellent cycleability, as compared to commercial carbon/graphite materials, has been extensively attempted to meet the new need such as electric vehicles (EVs) industry. Spinel $Li_4Ti_5O_{12}$ is considered as an alternative anode material [1,2] for lithium-ion batteries due to its appealing features such as "zero-strain" structure characteristic, high safety feature and flat charge–discharge voltage plateau. It has a stable operating voltage of about 1.55 V vs. Li/Li^+. Therefore, in principle, a cell with an operating voltage of about 2.5 V can be provided when $Li_4Ti_5O_{12}$ couples with high-voltage cathode materials such as $LiCoO_2$, $LiNiO_2$, $LiMn_2O_4$ and a 2 V cell can be yielded when it couples with $LiFePO_4$. In addition, $Li_4Ti_5O_{12}$ can also be applied in lithium metal rechargeable batteries [3,4], asymmetric supercapacitors [5,6], etc.

However, $Li_4Ti_5O_{12}$ has a low electric conductivity. Several methods have been utilized to improve the electric conductivity of $Li_4Ti_5O_{12}$, such as the formation of unique structure [7,8], reducing particle size [9,10], doping $Li_4Ti_5O_{12}$ with other metals or metal oxides [11,12], and coating $Li_4Ti_5O_{12}$ with conductive carbons [13–18]. In these methods, deposition of carbon on $Li_4Ti_5O_{12}$ particle surface has been proved as an effective way to improve the electric conductivity of the material. Xia et al. [13] synthesized a carbon-coated nanostructure $Li_4Ti_5O_{12}$ via a solid-state reaction using carbon-coated TiO_2 and Li_2CO_3. Gao et al. [17] synthesized a spherical $Li_4Ti_5O_{12}$/C composite via an "outer gel" method using $TiOCl_2$, NH_3 and carbon black as raw materials. Dominko et al. [18] prepared a $Li_4Ti_5O_{12}$/C composite using nano-titania coated a thin carbon film as precursor. It was observed that the $Li_4Ti_5O_{12}$/C obtained from all synthetic methods showed enhanced electrochemical performance. In addition, $Li_4Ti_5O_{12}$/C derived from other carbon sources such as sugar [19,20] and polymers [21,22] were examined. The added carbon, act as conductive network for $Li_4Ti_5O_{12}$ active particles, effectively improve the electrical contact of each $Li_4Ti_5O_{12}$ particle, thus enhancing electrochemical performances of $Li_4Ti_5O_{12}$.

However, previous studies [13–23] mainly focused on the synthesis of $Li_4Ti_5O_{12}$/C composite materials by adding adscititious carbon source. In this work, spinel $Li_4Ti_5O_{12}$/C composite was synthesized from PAALi and TiO_2 via one-step solid-state reaction without adscititious carbon source. Herein, PAALi was proposed to

* Corresponding author at: Chengdu Institute of Organic Chemistry, Chinese Academy of Sciences, Chengdu, Sichuan 610041, PR China. Tel.: +86 28 85229252; fax: +86 28 85233426.
E-mail address: zhdeng@cioc.ac.cn (Z.H. Deng).

0925-8388/$ – see front matter © 2010 Elsevier B.V. All rights reserved.
doi:10.1016/j.jallcom.2010.06.165

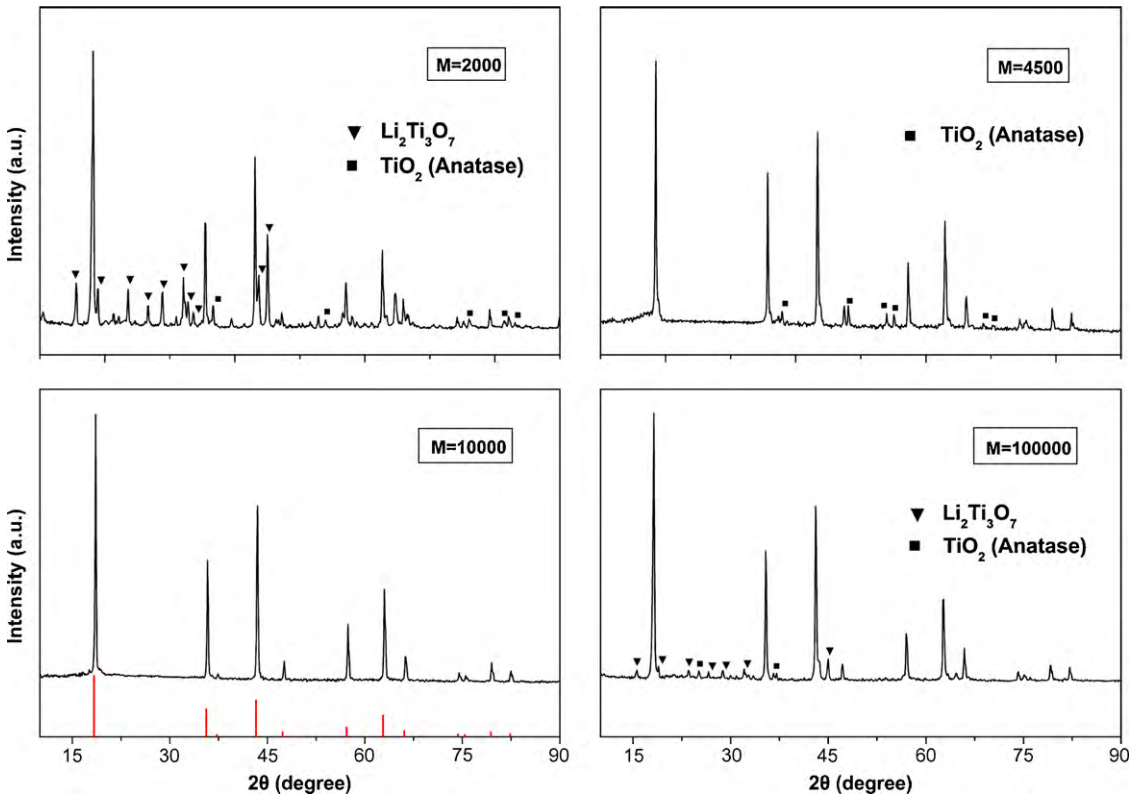

Fig. 1. XRD patterns of as-prepared $Li_4Ti_5O_{12}$/C from PAA with different molecular weights (red line means the standard $Li_4Ti_5O_{12}$). (For interpretation of the references to colour in this figure legend, the reader is referred to the web version of the article.)

be both the lithium and carbon sources. It is favorable to mix well, react completely and get homogenous $Li_4Ti_5O_{12}$/C samples because no extra carbon source was added. The physical and electrochemical properties of the $Li_4Ti_5O_{12}$/C samples derived from PAA with different molecular weights (mol. wts.), different heating rates and sintering durations were examined. Moreover, the electrochemical performances of the $Li_4Ti_5O_{12}$/C sample prepared at optimized synthesis conditions were tested.

2. Experimental

2.1. Preparation of $Li_4Ti_5O_{12}$/C composites

A stoichiometric amount of $LiOH{\cdot}H_2O$ was dissolved into aqueous solutions of polyacrylic acid (PAA, M = 2000, 4500, 10,000, 100,000) with the molar ratio of 1:1. Then powdered TiO_2 (Li:Ti = 4:5) was added into the PAALi solutions with continuous stirring for 6 h to yield homogeneous PAALi + TiO_2 slurries. Subsequently, the above mixtures were dried, sintered at 800 °C for 4–12 h in flowing nitrogen with heating rate of 5–25 °C min^{-1}, followed by cooling down to room temperature slowly. The final $Li_4Ti_5O_{12}$/C samples were obtained by grinding.

2.2. Cells assembly and performance evaluation

Electrochemical properties of the $Li_4Ti_5O_{12}$/C composites were evaluated using 2032 coin cells with a lithium metal foil as the counter electrode. The $Li_4Ti_5O_{12}$/C working electrodes were made by mixing active materials, conductive carbon black (Super P, TIMCAL) and an aqueous binder LA132 (Indigo, China) in a weight ratio of 86:10:4, and then pasted uniformly onto a copper foil and dried at a temperature of 120 °C to give the electrodes. All electrodes were cut into disks with a diameter of 1.45 cm (thus the area of 1.65 cm^2), pressed, dried at 90 °C under vacuum for 6 h, and then stored in an argon-filled dry box. The cells were assembled in an argon-filled dry glove box. The electrolyte was a 1.0 M $LiPF_6$ solution in the mixture of ethylene carbonate, dimethyl carbonate and ethylene methyl carbonate (1:1:1 by volume). A Celgard 2400 polypropylene membrane was used as the separator.

X-ray diffraction (XRD) of $Li_4Ti_5O_{12}$/C was carried on a Rigaku D/Max 2550 powder diffractometer with Cu-Kα radiation of λ = 1.5418 Å in the range of $10° < 2\theta < 90°$. Scanning electron microscopy (SEM) was conducted on a JEOL JSM-6700F scanning electron microscope. Transmission electron microscopy (TEM) was revealed by a JEOL JEM-3010 transmission electron microscope. The amount of carbon in $Li_4Ti_5O_{12}$/C composite was measured by thermogravimetric-differential thermal analysis (TG/DTA) methods with scanning rate of 10 °C min^{-1} in air atmosphere from 25 to 800 °C, by a Netzsch STA409PC thermal analyzer. The particle size distribution was identified by a BT-2003 laser particle size analyzer. Constant current charge–discharge and cycle performance of the cells were tested on a Neware Battery Tester and cyclic voltammograms were investigated by an Arbin Instrument. All the tests were carried out at room temperature.

3. Results and discussion

3.1. XRD analysis

Fig. 1 shows the XRD patterns of as-prepared spinel $Li_4Ti_5O_{12}$/C using PAALi with different mol. wts. As is seen in the figure, the crystal structure of the samples is greatly changed with molecular weight (mol. wt.) of PAA. When the mol. wt. of the PAA is 10,000 (Fig. 1c), the XRD diagram of the $Li_4Ti_5O_{12}$/C shows the absence of parasitic peaks, and it is in good accordance with the standard $Li_4Ti_5O_{12}$ pattern (PDF no. 26-1198), demonstrating that a single phase is obtained with no evidence of other lithium titanates with different crystal structure in the composite and the carbon from PAALi does not greatly affect the structure of $Li_4Ti_5O_{12}$. When the PAA with mol. wt. of 2000, 4500 and 100,000 are adopted, all the samples show the impurity phase peaks, as shown in Fig. 1a, b and d. When the mol. wt. of PAA is too small (e.g. 2000), the obtained PAALi would be fluid due to fusing like small-molecule inorganic lithium-salts when be sintered. Flow of PAALi induces surface segregation phenomena between PAALi melt phase and TiO_2 solid phase, which results in poor uniformity of the precursor mixtures. Therefore, lithium titanates with different ratios of Li/Ti would yield where the lithium salt is enriched or lacking. Therefore, the final sample is the eutectic mixture of $Li_4Ti_5O_{12}$, $Li_2Ti_3O_7$ and TiO_2. When the mol. wt. of PAA is 4500, there is a small amount of impurity phase

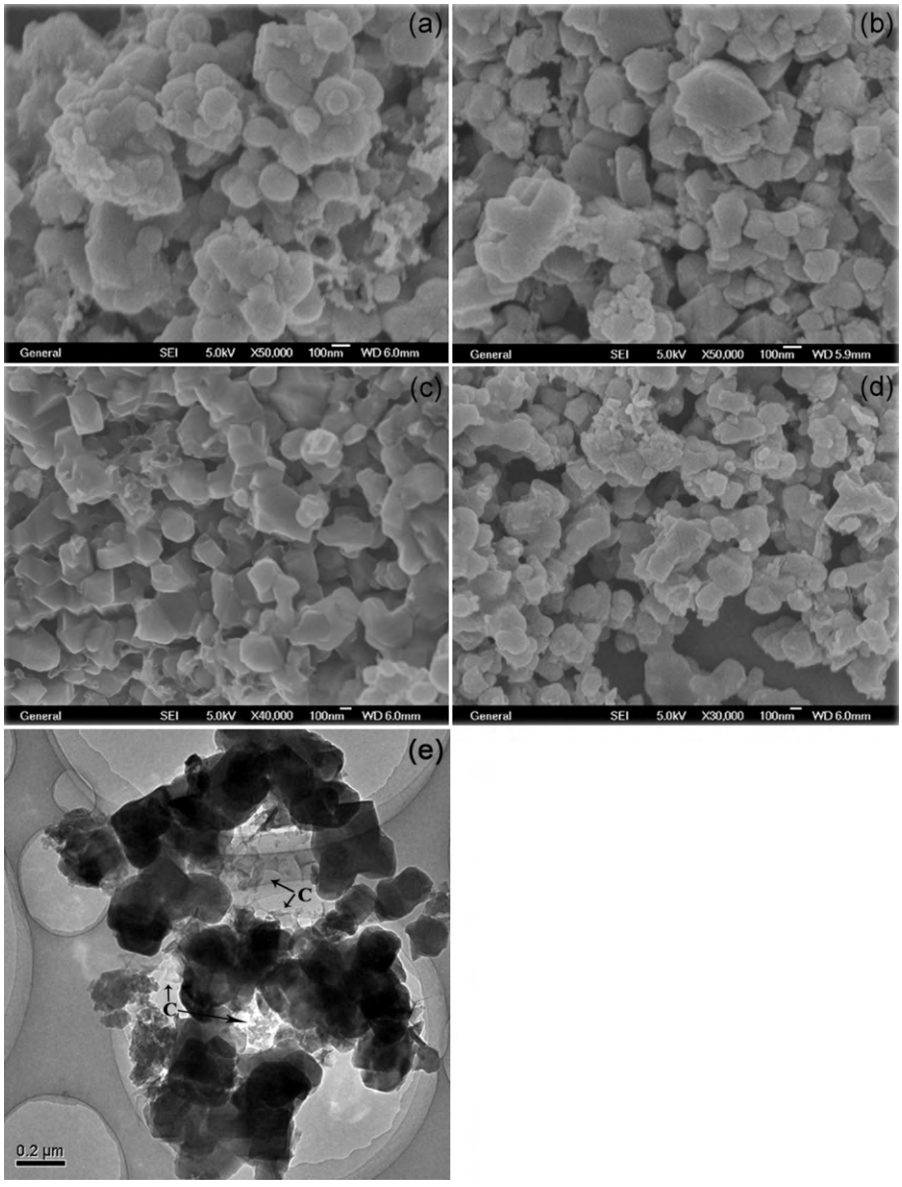

Fig. 2. $Li_4Ti_5O_{12}$/C derived from different molecular weight PAA 2000 (a), 4500 (b), 10,000 (c), 100,000 (d) of SEM images, and TEM image of $Li_4Ti_5O_{12}$/C (e).

anatase TiO_2. When the mol. wt. of PAA is too large (e.g. 100,000), the obtained PAALi would disperse non-homogeneously in precursor mixtures due to the effect of polymer framework, hence resulting in excessive or insufficient PAALi content at partial areas. Thereby, the eutectic mixture of $Li_4Ti_5O_{12}$, $Li_2Ti_3O_7$ and TiO_2 is also obtained.

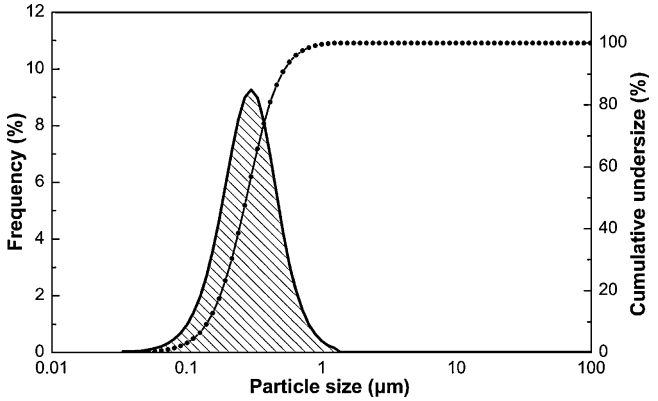

Fig. 3. The particle size distribution of $Li_4Ti_5O_{12}$/C.

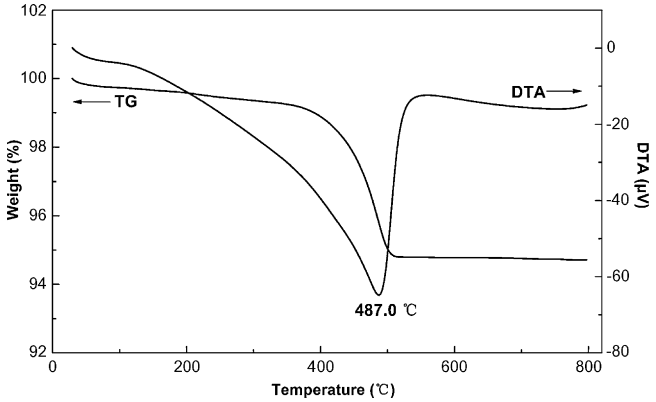

Fig. 4. TG–DTA curves of $Li_4Ti_5O_{12}$/C.

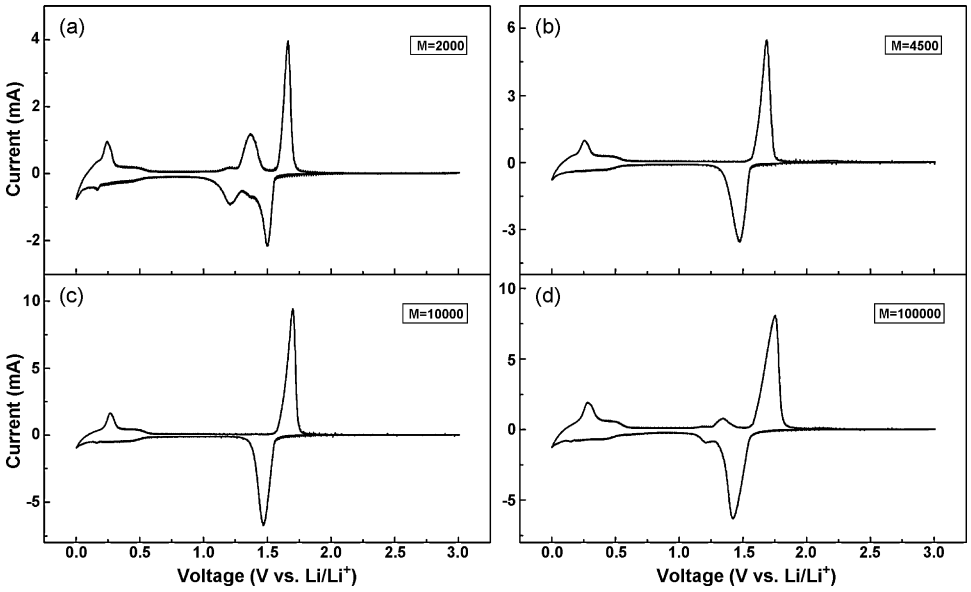

Fig. 5. CVs of the $Li_4Ti_5O_{12}$/C electrodes from PAALi with different molecular weights.

3.2. Electron microscopy, particle size distribution and TG/DTA analysis

Fig. 2a–d shows the SEM pictures of $Li_4Ti_5O_{12}$/C derived from PAALi with different mol. wts. The samples mainly display regular crystalline morphology when the mol. wts. of PAA are 4500 and 10,000. The crystalline morphology of the sample is the most regular when the mol. wt. of PAA is 10,000 (Fig. 2c). Otherwise, as revealed in Fig. 2a and d, the samples demonstrate the crystalline morphology of not only $Li_4Ti_5O_{12}$ but also impurities when PAA with the mol. wts. of 2000 and 100,000 are used, which indicates other lithium titanates or carbon exists in $Li_4Ti_5O_{12}$/C samples. The above results of SEM images illustrate that the samples display regular crystalline morphology and no other lithium titanates exist when the mol. wts. of PAA are 4500 and 10,000, which is consistent with the results of XRD patterns. Fig. 2e presents the TEM photograph of $Li_4Ti_5O_{12}$/C derived from PAA with mol. wt. of 10,000. It can be clearly seen from the figure that most $Li_4Ti_5O_{12}$ parti-

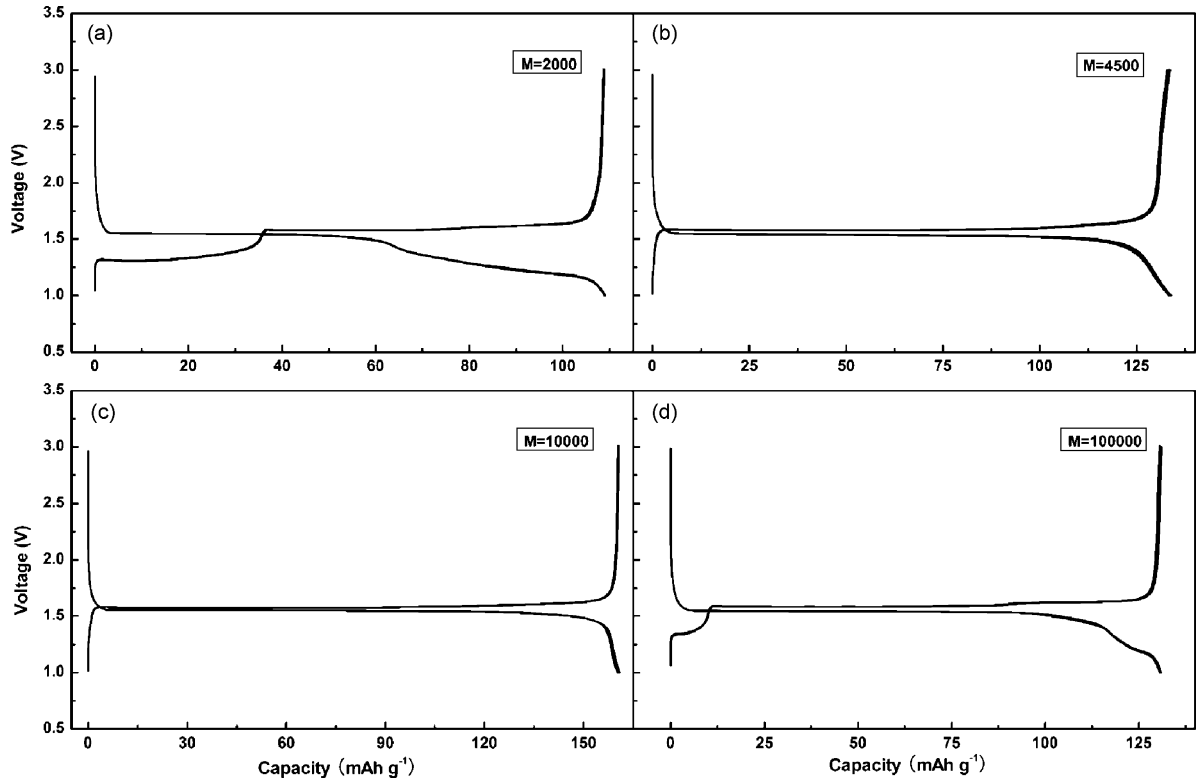

Fig. 6. Constant current charge–discharge curves of the $Li_4Ti_5O_{12}$/C electrodes from PAALi with different molecular weights.

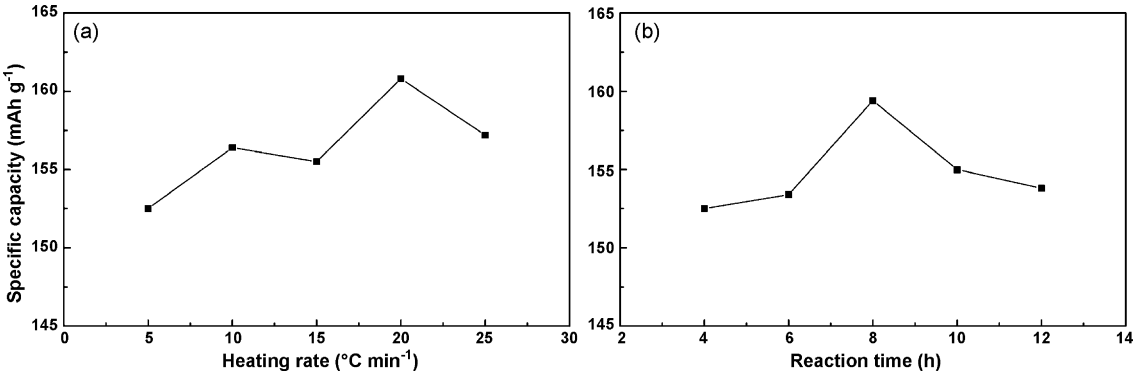

Fig. 7. Specific capacities of as-prepared $Li_4Ti_5O_{12}$/C sintered under different heating rates (a), different heating durations (b).

cles are wrapped with carbon webs [24]. The connection between $Li_4Ti_5O_{12}$ and pyrolytic carbon is tight, which is profitable to the improvement of electronic conductivity. The electronic conductivity of $Li_4Ti_5O_{12}$/C samples as shown in Fig. 2a–d reaches 2.7×10^{-7}, 2.9×10^{-7}, 2.9×10^{-7} and 3.0×10^{-7} S cm^{-1}, respectively. It is seen in Fig. 3 the particle size distribution of the $Li_4Ti_5O_{12}$/C derived from PAA with mol. wt. of 10,000 is narrow and the average particle size is 280 nm, which is consistent with the results of TEM image. The content of carbon in the composite $Li_4Ti_5O_{12}$/C derived from PAA with mol. wt. of 10,000 is 4.66% measured by TG/DTA method, as shown in Fig. 4.

3.3. Cyclic voltammetry

Fig. 5 shows the cyclic voltammograms (CVs) of the $Li_4Ti_5O_{12}$/C electrodes from PAALi with different mol. wts. The CVs' voltage ranges of all electrodes are 0–3.0 V, and the scan rates are all 0.2 mV s^{-1}. It is obvious that four samples show two pairs of redox peaks, the first pair of redox peaks is the characteristics redox peaks of $Li_4Ti_5O_{12}$ (1.70 and 1.46 V), the second pair of redox peaks is attributed to the carbon component in the $Li_4Ti_5O_{12}$/C composite (below 1.0 V) [25]. However, there is a third pair of redox peaks that is located at 1.37 and 1.20 V, as shown in Fig. 5a and d. It is proved that the third pair of redox peaks is caused by oxidation–reduction behavior of $Li_2Ti_3O_7$ [26]. These facts are consistent with the results of XRD patterns.

3.4. Electrochemical measurements

Fig. 6 shows the constant current charge–discharge curves of the $Li_4Ti_5O_{12}$/C electrodes from PAALi with different mol. wts. The charge–discharge test is carried out at a current density of 0.86 mA cm^{-2} (1 C). As shown in Fig. 6a and d, the appearance of a characteristic plateau different from $Li_4Ti_5O_{12}$ is due to $Li_2Ti_3O_7$. It is confirmed that there are impurity phase $Li_2Ti_3O_7$ in $Li_4Ti_5O_{12}$/C composites when the PAA with the mol. wt. of 2000 and 100,000 are adopted. These facts are consistent with the results of XRD patterns and CVs curves. However, as revealed in Fig. 6b and c, the typical characteristic plateau of $Li_4Ti_5O_{12}$ is obtained, where the mol. wt. of PAA is 4500 and 10,000, respectively. It is clear that the $Li_4Ti_5O_{12}$/C electrode has a higher capacity when the mol. wt. of PAA is 10,000.

The above results show that the mol. wt. of PAA is an important factor for the synthesis of spinel $Li_4Ti_5O_{12}$/C. The physical and electrochemical performances of as-prepared $Li_4Ti_5O_{12}$/C are influenced greatly by the mol. wt. of PAA. The increase of the mol. wt. increases the distribution homogeneity of lithium source in precursors when be heat-treated. However, on the other hand, the increase of the mol. wt. increases the dispersion inhomogeneity of PAALi in precursors because of the effect of polymer framework of PAA. The both extreme choice would lead to failure to synthesize the purity phase $Li_4Ti_5O_{12}$/C. Therefore, the PAA with mol. wt. of 10,000 is chosen as the optimum value for the synthesis of regular crystalline morphology and purity phase $Li_4Ti_5O_{12}$/C composite.

The heating rate and sintering duration are another two important influence factors on the electrochemical performances of $Li_4Ti_5O_{12}$/C. Fig. 7a shows the reversible capacities of as-prepared $Li_4Ti_5O_{12}$/C sintered at 800 °C with different heating rates and PAA with the mol. wt. of 10,000. It is seen from the figure that the maximum reversible capacity is reached at heating rate of 20 °C min^{-1}. The reason may be that vacancies left by small volatile molecules when heat-treatment can be kept in the formed product and result in an increase of micropores. The micropores are effective places for lithium storage [27,28]. Moreover, the interconnected microstructure helps the electrolyte to equably penetrate the electro-active materials, which leads to better electrochemical performance of $Li_4Ti_5O_{12}$/C. At higher heating rates (>20 °C min^{-1}), the in-situ pyrolyzed PAA form a large number of small and interconnected pores. However, excessive pores result in an increase of "dead lithium", which affects reversible capacity of $Li_4Ti_5O_{12}$/C. At lower heating rates (<20 °C min^{-1}), large but separated pores are mainly formed because of small volatile molecules escaping from solid samples at lower speed, which is unfavorable for the electrolyte to equably penetrate the electro-active materials. Therefore, the heating rate of 20 °C min^{-1} is an optimum value for the synthesis of spinel $Li_4Ti_5O_{12}$/C. Fig. 8 shows the constant current charge–discharge curves of the $Li_4Ti_5O_{12}$/C in Fig. 7a. Fig. 7b shows the reversible capacities of as-prepared $Li_4Ti_5O_{12}$/C sintered at 800 °C under different sintering durations with the heating rate of 20 °C min^{-1} and PAA with the mol. wt. of 10,000. It is seen from the figure that the maximum reversible capacity is obtained at sintering duration of 8 h. It is well known that crystal integrality and granularity of products are considered to be the main factors affecting the electrochemical performances. When the sintering duration is shortened, single-phase $Li_4Ti_5O_{12}$ or products with complete crystal structure may not be obtained, which leads to the instability of crystal and causes bad influence on the electrochemical performances of the products. When the sintering duration is increased, it is unfavorable for Li^+ diffusing in crystal due to the increase of particle size and the decrease of specific surface area, which also affects the electrochemical performances of the products. Therefore, the sintering duration of 8 h is chosen as the optimum value for the synthesis of $Li_4Ti_5O_{12}$/C composite. Fig. 9 shows the constant current charge–discharge curves of the $Li_4Ti_5O_{12}$/C in Fig. 7b.

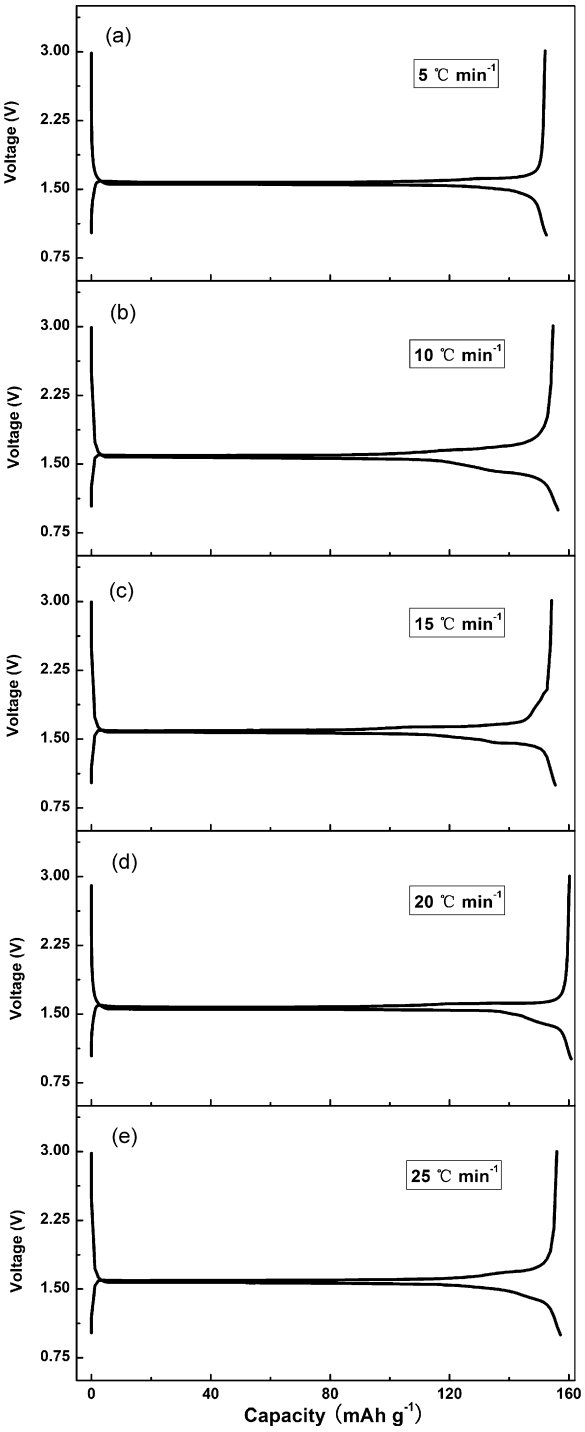

Fig. 8. Constant current charge–discharge curves of the $Li_4Ti_5O_{12}$/C in Fig. 7a.

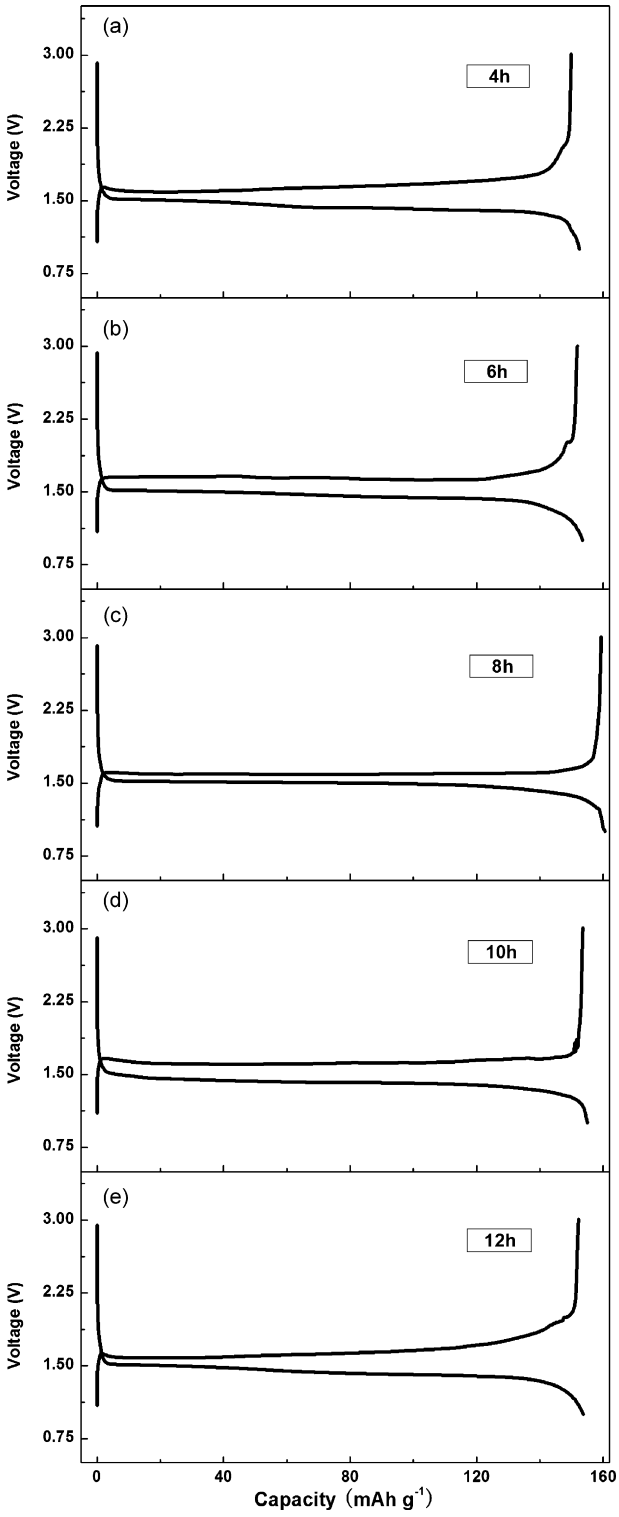

Fig. 9. Constant current charge–discharge curves of the $Li_4Ti_5O_{12}$/C in Fig. 7b.

Fig. 10 shows the cycle curves of as-prepared $Li_4Ti_5O_{12}$/C at the optimum values of PAA with the mol. wt. of 10,000, heating rate of 20 °C min^{-1} and sintering duration of 8 h. The constant current charge–discharge curves of as-prepared $Li_4Ti_5O_{12}$/C at high rates are shown in Fig. 11. It can be seen that $Li_4Ti_5O_{12}$/C has good cycle stability though the reversible capacities decreased gradually with the increase of current density. At 0.2 C, the initial capacity is 162.2 mAh g^{-1} with capacity retention of 99.34% at 50th cycle. At 4 C and 8 C, the initial capacity is 148.4 and 142.4 mAh g^{-1} with capacity retention of 94.48 and 90.53% at 50th cycle, respectively. Moreover, even at 20 C the initial capacity is 116.0 mAh g^{-1} with capacity retention of 87.61% at 50th cycle. However, at 20 C, polarization of the cell is very obvious, and noticeably, its discharge voltage platform significantly drops. The results show that $Li_4Ti_5O_{12}$/C composite has good cycle life performance at high rates.

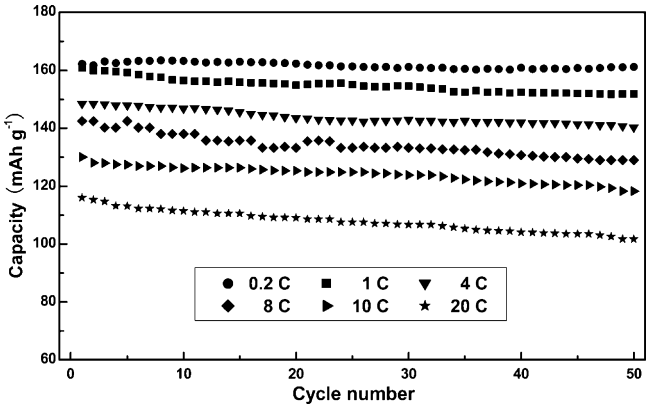

Fig. 10. Cycleabilities of $Li_4Ti_5O_{12}$/C derived from optimized synthesis conditions at various rates.

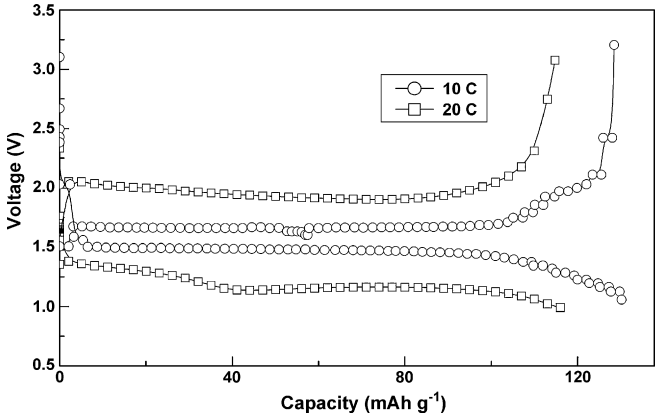

Fig. 11. Constant current charge–discharge curves of as-prepared $Li_4Ti_5O_{12}$/C at high rates.

4. Conclusions

In this work, spinel $Li_4Ti_5O_{12}$/C was obtained from PAALi and TiO_2 via one-step solid-state reaction without adscititious carbon sources. Herein, the PAALi supplies both lithium and carbon sources. The mol. wt. of PAA, heating rate and sintering duration directly affect the physical and electrochemical performances of $Li_4Ti_5O_{12}$/C. The results demonstrate that the mol. wt. of PAA, heating rate and sintering duration is optimized to be 10,000, 20 °C min^{-1} and 8 h, respectively, at which the $Li_4Ti_5O_{12}$/C shows the initial capacity of 148.4 mAh g^{-1} with 5.52% capacity fading after 50 cycles at 4 C, and 142.4 mAh g^{-1} with 9.47% capacity fading after 50 cycles at 8 C. An initial capacity 116.0 mAh g^{-1} with a capacity fading of 12.39% after 50 cycles is obtained even at 20 C. The $Li_4Ti_5O_{12}$/C composite derived from this synthetic route shows good rate cyclic performance and will be a very promising material to be used in high-rate lithium-ion batteries.

References

[1] K. Tokumitsu, A. Mabuchi, H. Fujimoto, J. Power Sources 54 (1995) 444–447.
[2] Y. Matsumura, S. Wang, J. Mondori, J. Electrochem. Soc. 142 (1995) 2914–2918.
[3] J. Morales, R. Trócoli, S. Franger, J. Santos-Pena, Electrochim. Acta 55 (2010) 3075–3082.
[4] N.A. Alias, M.Z. Kufian, L.P. Teo, S.R. Majid, A.K. Arof, J. Alloys Compd. 486 (2009) 645–648.
[5] L. Cheng, H.J. Liu, J.J. Zhang, H.M. Xiong, Y.Y. Xia, J. Electrochem. Soc. 153 (2006) A1472–A1477.
[6] A.D. Pasquier, A. Laforgue, P. Simon, J. Power Sources 125 (2004) 95–102.
[7] N.Y. He, B.S. Wang, J.J. Huang, J. Solid State Electrochem. 14 (2010) 1241–1246.
[8] C. Lai, Y.Y. Dou, X. Li, X.P. Gao, J. Power Sources 195 (2010) 3676–3679.
[9] A.S. Prakash, P. Manikandan, K. Ramesha, M. Sathiya, J.-M. Tarascon, A.K. Shukla, Chem. Mater. 22 (2010) 2857–2863.
[10] M.W. Raja, S. Mahanty, M. Kundu, R.N. Basu, J. Alloys Compd. 468 (2009) 258–262.
[11] X. Li, M.Z. Qu, Z.L. Yu, J. Alloys Compd. 487 (2009) L12–L17.
[12] T.F. Yi, J. Shu, Y.R. Zhu, X.D. Zhu, R.S. Zhu, A.N. Zhou, J. Power Sources 195 (2010) 285–288.
[13] L. Cheng, J. Yan, G.N. Zhu, J.Y. Luo, C.X. Wang, Y.Y. Xia, J. Mater. Chem. 20 (2010) 595–602.
[14] T. Yuan, X. Yu, R. Cai, Y.K. Zhou, Z.P. Shao, J. Power Sources 195 (2010) 4997–5004.
[15] T. Yuan, R. Cai, R. Ran, Y.K. Zhou, Z.P. Shao, J. Alloys Compd. (2010), doi:10.1016/j.jallcom.2010.04.253.
[16] Y.J. Hao, Q.Y. Lai, J.Z. Lu, D.Q. Liu, X.Y. Ji, J. Alloys Compd. 439 (2007) 330–336.
[17] J. Gao, J.R. Ying, C.Y. Jiang, C.R. Wan, J. Power Sources 166 (2007) 255–259.
[18] R. Dominko, M. Gaberscek, M. Bele, J. Eur. Ceram. Soc. 27 (2007) 909–913.
[19] J.B. Kim, D.J. Kim, K.Y. Chung, D.J. Byun, B.W. Cho, Phys. Scr. T139 (2010) 014026.
[20] G.J. Wang, J. Gao, L.J. Fu, N.H. Zhao, Y.P. Wu, T. Takamura, J. Power Sources 174 (2007) 1109–1112.
[21] H. Liu, Y. Feng, K. Wang, J.Y. Xie, J. Phys. Chem. Solids 69 (2008) 2037–2040.
[22] H.Y. Yu, X.F. Zhang, A.F. Jalbout, X.D. Yan, X.M. Pan, H.M. Xie, R.S. Wang, Electrochim. Acta 53 (2008) 4200–4204.
[23] L.X. Yang, L.J. Gao, J. Alloys Compd. 485 (2009) 93–97.
[24] H.T. Chung, S.K. Jang, H.W. Ryu, K.B. Shim, Solid State Commun. 131 (2004) 549–554.
[25] K. Sawai, Y. Iwakoshi, T. Ohzuku, Solid State Ionics 69 (1994) 273–283.
[26] M.V. Thournout, A. Picard, M. Womes, J.O. Fourcade, J.C. Jumas, J. Phys. Chem. Solids 67 (2006) 1355–1358.
[27] A. Mabuchi, K. Tokumitsu, H. Fujimoto, T. Kasuh, J. Electrochem. Soc. 142 (1995) 1041–1046.
[28] G. Sandí, R.E. Winans, K.A. Carrado, J. Electrochem. Soc. 143 (1996) L95–L98.